β-Hairpin nucleation by Pro-Gly β-turns. Comparison of D-Pro-Gly and L-Pro-Gly sequences in an apolar octapeptide

Srinivasa Rao Raghothama,[a] Satish Kumar Awasthi[b] and Padmanabhan Balaram*[,b]

Molecular Biophysics Unit[b] and Sophisticated Instruments Facility,[a] Indian Institute of Science, Bangalore-560012, India

The solution conformation of the synthetic octapeptide Boc-Leu-Val-Val-D-Pro-Gly-Leu-Val-Val-OMe 1 and Boc-Leu-Val-Val-Pro-Gly-Leu-Val-Val-OMe 2 have been investigated in organic solvents by NMR spectroscopy. Peptide 1 adopts well-defined β-hairpin conformations in $CDCl_3$, C_6D_6 and $(CD_3)_2SO$, nucleated by a D-Pro-Gly Type II′ β-turn, as demonstrated by the observation of characteristic nuclear Overhauser effects (NOEs) between backbone protons and solvent shielding of NH groups involved in cross-strand hydrogen bonding. Chemical shifts and coupling constants provide further support for the β-hairpin conformation, which is consistent with the observation of a single negative circular dichroism band at 216 nm in methanol. In peptide 2, there is no characteristic interstrand NOE observed in $(CD_3)_2SO$, while in $CDCl_3$ pronounced aggregation results in line broadening. The observation of a low temperature coefficient for the Leu(6)NH proton favours a population of Pro-Gly Type II β-turn conformations. These results suggest that in short peptide sequences, the precise nature of the β-turn is critical for hairpin formation, with Type II′ β-turns being particularly effective.

β-Hairpins are widely occurring secondary structure elements in proteins.[1,2] Several recent investigations have focussed on the design of stable β-hairpins in synthetic peptide sequences.[3–10] Hairpin formation in polypeptide chains is nucleated by chain reversals facilitated by β-turns or short loop segments. Cross-strand hydrogen bonding stabilizes β-hairpin structures. Analyses of β-hairpin structures in proteins reveal that the most common nucleating turns are Type I′ and II′ turns.[1,2,11] (β-Turns are characterized by the Ramachandran angles at residues $i + 1$ and $i + 2$: Type I′, $\varphi_{i+1} = +60°$, $\psi_{i+1} = +30°$, $\varphi_{i+2} = 90°$, $\psi_{i+2} = 0°$; Type II′, $\varphi_{i+1} = 60°$, $\psi_{i+1} = -120°$, $\varphi_{i+2} = -80°$, $\psi_{i+2} = 0°$).[12–14] In both of these types φ_{i+1} is positive and lies in a region of conformational space which is very poorly populated by L-amino acids, as a consequence of steric limitations.[15] In protein structures, the achiral residue Gly is most often found at the $i + 1$ position of Type I′/II′ β-turns.[13] Less frequently, Asn residues, with a significant propensity for positive φ values are also observed at this position.[16]

De novo design of synthetic protein structures requires the design and construction of stable elements for the secondary structure.[17,18] As part of an approach to the modular construction of synthetic protein mimics, we have been investigating strategies for the synthesis of stable β-hairpin peptides. Our approach relies on the use of the D-Pro residue to nucleate Type I′/II′ β-turns,[19–23] since the constraints of pyrrolidine ring formation restrict the φ value in D-Pro to $+60 \pm 20°$. We have earlier described in a preliminary communication[22] the formation of a β-hairpin structure in solution for the peptide Boc-Leu-Val-Val-D-Pro-Gly-Leu-Val-Val-OMe **1** and established a β-hairpin conformation in single crystals by X-ray diffraction.[23] In this report we present a detailed NMR characterization of the β-hairpin conformation of **1** in diverse solvents and provide a comparison of the conformational properties of this peptide with the corresponding L-Pro analog, Boc-Leu-Val-Val-Pro-Gly-Leu-Val-Val-OMe **2**.

Results

NMR study of Boc-Leu-Val-Val-D-Pro-Gly-Leu-Val-Val-OMe (1)

The conformation of **1** was investigated by NMR spectroscopy in three deuterated solvents: chloroform ($CDCl_3$), benzene (C_6D_6) and dimethyl sulfoxide $(CD_3)_2SO$. While peptide **1** was readily soluble in $CDCl_3$ and $(CD_3)_2SO$ at the concentrations investigated (up to 24 mM), a slightly turbid solution was obtained in C_6D_6 at a concentration of 8 mM, which was completely clarified by the addition of 1.7% $(CD_3)_2SO$. In all three solvents sharp, well-resolved resonances were observed at concentrations ranging from 0.2 to 24 mM, with no significant concentration dependence of NH chemical shifts, suggesting that aggregation effects are unimportant. Sequence specific assignments of backbone NH and $C^{\alpha}H$ resonances were readily achieved by a combination of DQFCOSY and ROESY experiments.[24] The relevant chemical shifts are summarized in Table 1.

Fig. 1 shows the large dispersion of NH chemical shifts in C_6D_6 with several NH resonances appearing at very low field (>8 ppm), indicative of well-defined conformations in solution. The high $^3J_{NH-C^{\alpha}H}$ value (>8 Hz) for the residues 1–3 and 6–8 also provide supporting evidence for strand conformations ($\psi \sim 120°$) for these segments in all three solvents.

Conformation in C_6D_6. Fig. 1 shows the partial ROESY spectrum of **1** in C_6D_6, illustrating $C^{\alpha}H \leftrightarrow NH$ NOEs. It is clearly seen that the inter-residue NOEs $C_i^{\alpha}H \leftrightarrow N_{i+1}H$ are much more intense than the intra-residue $C_i^{\alpha}H \leftrightarrow N_iH$. This agrees with an extended conformation for segments 1–3 and 6–8. Note that the Gly(5)$C^{\alpha}H \leftrightarrow$Leu(6)NH NOE is extremely weak, with only the high-field Gly(5)$C^{\alpha}H$ proton showing a very weak connectivity. This observation favours a folded conformation at Gly(5). Only three very weak NH↔NH NOEs were detected between residues Leu(1)↔Val(2), Gly(5)↔Leu(6) and Val(3)↔Leu(6). The last two NOEs are clearly diagnostic of a β-hairpin conformation, shown in Fig. 2. Indeed, the Gly(5)NH↔Leu(6)NH NOE supports a helical conformation at Gly(5) ($\varphi \pm 60° \pm 30°$, $\psi \pm 40° \pm 30°$). Together with the strong $d_{\alpha N}$ NOE between Pro(4)$C^{\alpha}H$ and Gly(5)NH, these results strongly support a Type II′ β-turn conformation for the D-Pro-Gly segments. The observed Val(3)NH↔Leu(6)NH NOEs confirms extension of the β-hairpin. Definitive support for the β-hairpin conformation of peptide **1** in C_6D_6 is obtained from cross-strand Val(2)$C^{\alpha}H \leftrightarrow$Val(7)$C^{\alpha}H$ NOEs (Fig. 3). Temperature coefficients of NH chemical shifts in deuterated benzene (Table 1)

Table 1 NMR parameters for peptide Boc-Leu-Val-Val-D-Pro-Gly-Leu-Val-Val-OMe, **1**

Solvent	Leu(1)	Val(2)	Val(3)	D-Pro(4)	Gly(5)	Leu(6)	Val(7)	Val(8)
NH chemical shift								
C_6D_6 [a]	6.36	8.04	9.21	—	7.36	8.10	8.43	8.81
$CDCl_3$	5.62	6.54	8.73	—	6.13	7.65	6.44	8.33
DMSO [b,c]	6.84	7.78	8.39		8.18	7.75	8.26	8.22
	(7.04)	(7.54)	(8.03)	—	(8.22)	(7.96)	(7.86)	(8.07)
	[7.03]	[7.50]	[7.99]		[8.19]	[7.70]	[7.77]	[8.02]
$C^{\alpha}H$ chemical shift								
C_6D_6 [a]	4.65	5.26	4.78	4.27	4.39; 3.82	5.18	5.07	4.90
$CDCl_3$	4.09	4.74	4.54	4.33	3.97	4.46	4.69	4.56
DMSO [b,c]	4.03	4.53	4.36	4.27	3.70; 3.47	4.51	4.33	4.18
	(3.96)	(4.24)	(4.00)	(4.86)	(3.78; 3.64)	(4.39)	(4.22)	(4.13)
	[3.95]	[4.26]	[4.28]	[4.27]	[3.68]	[4.36]	[4.23]	[4.13]
$^3J_{NHC^{\alpha}H}$/Hz								
C_6D_6 [a]	9.0	9.5	9.4	—	—	8.9	8.6	8.6
$CDCl_3$	8.5	9.1	9.0	—	—	8.0	8.6	8.0
DMSO [b,c]	8.8	9.1	8.5			8.8	8.8	8.4
	(8.4)	(9.0)	(7.8)	—	—	(8.4)	(8.7)	(7.8)
	[8.4]	[8.9]	[8.6]			[8.1]	[8.8]	[7.7]
$(d\delta/dT)$/ppb K^{-1}								
C_6D_6 [a]	10.8	12.5	7.4	—	13.9	5.5	18.0	10.2
$CDCl_3$	4.3	0.3	4.0	—	−0.4	2.9	1.1	7.2
DMSO [b,c]	4.7	4.9	5.4		5.6	2.0	7.2	5.5
	(6.6)	(3.1)	(5.2)	—	(—)	(4.1)	(4.4)	(5.5)
	[6.9]	[2.7]	[6.4]		[5.6]	[2.7]	[5.1]	[5.7]

[a] Contains ~1.7% DMSO. [b] Values for minor (*cis*) isomer are given within parentheses. [c] Values for peptide Boc-Leu-Val-Val-Pro-Gly-Leu-Val-Val-OMe are within square brackets.

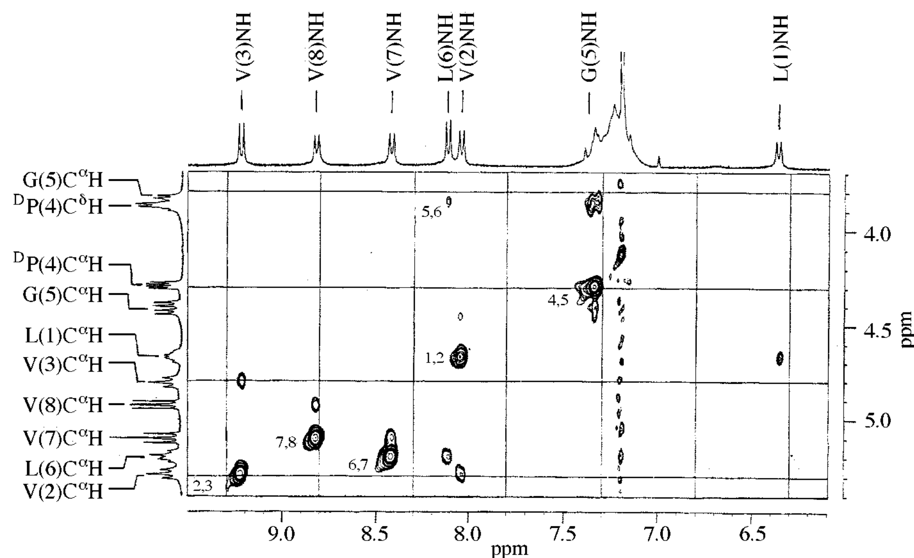

Fig.1 Partial $C^{\alpha}H$–NH ROESY spectra (400 MHz) of peptide **1** (D-Pro-Gly) in deuterated benzene (C_6D_6)

revealed distinctly low temperature dependences for the Val(3) and Leu(6) NH protons, both of which are internally hydrogen bonded in the β-hairpin shown in Fig. 2. Of the remaining residues, Leu(1) and Val(8) NH groups showed relatively lower temperature dependences, suggesting a greater degree of solvent shielding, consistent with their involvement of inter-strand interaction in the proposed β-hairpin conformation. It should be noted that the temperature coefficients in aromatic solvents, such as C_6D_6 must be interpreted with caution because of specific solvation effects.[25] The observation of a β-hairpin conformation in crystals[23] with nearly ideal interstrand hydrogen bonding lends additional support to the above interpretation of NMR data.

Conformation in $CDCl_3$. A schematic comparison of NH and $C^{\alpha}H$ chemical shifts in C_6D_6, $CDCl_3$ and $(CD_3)_2SO$ is provided in Fig. 4. The Val(3), Val(8) and Leu(6) groups remain at appreciably lower fields than the other NH resonances in $CDCl_3$, suggesting that the conformation shown in Fig. 2 is maintained in this solvent. The Val(3), Val(8) and Leu(6) NH groups are internally hydrogen bonded in the β-hairpin. It should be noted that Leu(1)NH appears at higher field because of the chemically distinct character of the urethane moiety in the Boc-protected *N*-terminus residues. In $CDCl_3$, no NH↔NH NOEs were detected, while medium and strong inter-residue $C^{\alpha}_{i}H$↔$N_{i+1}H$ NOEs were observed. The succession of $d_{\alpha N}$ NOEs 1↔2↔3 and 6↔7↔8 suggests the retention of the strand segments in the β-hairpin conformation, observed in C_6D_6. Solvent perturbation of NH chemical shifts, carried out by the addition of 0–20% (v/v) $(CD_3)_2SO$,[26] revealed that Val(3), Leu(6) and Val(8) NH groups are insensitive to perturbation, while Leu(1) showed a small downfield shift upon increasing $(CD_3)_2SO$ concentration. Much larger solvent chemical shifts

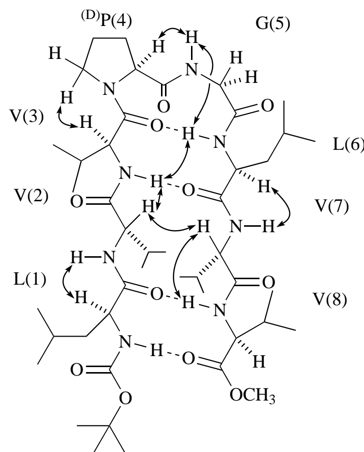

Fig. 2 Schematic diagram of a β-hairpin conformation for octapeptide **1** (D-Pro-Gly)

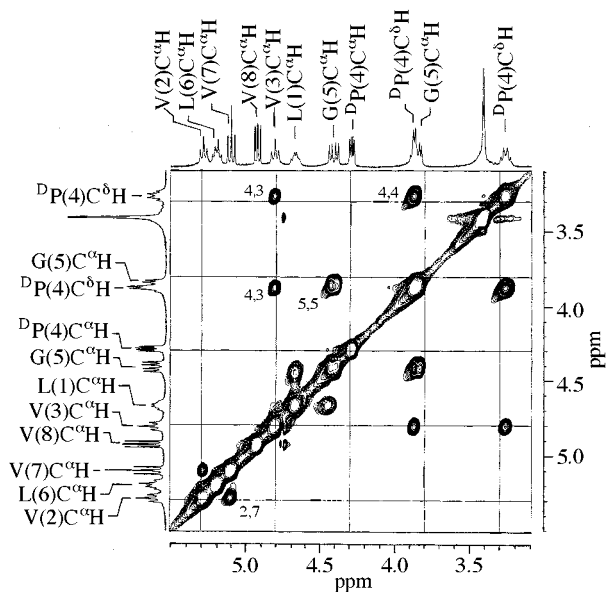

Fig. 3 Partial CαH–CαH ROESY spectra (400 MHz) of peptide **1** (D-Pro-Gly) in deuterated benzene (C_6D_6)

were observed for Gly(5), Val(2) and Val(7) NH resonances, a characteristic of exposed NH groups. These observations are broadly consistent with the β-hairpin shown in Fig. 2.

Fig. 5 shows the effect of addition of the paramagnetic aminoxyl radical 2,2,6,6-tetramethylpiperidine-1-oxyl (TEMPO)[27,28] on the NH linewidths in peptide **1**, in $CDCl_3$. Over the range of radical concentrations investigated, only Gly(5)NH shows dramatic line broadening, a feature anticipated in the β-hairpin conformation. Intriguingly, all remaining NH resonances are relatively insensitive to radical addition. While the four internally bonded resonances Leu(1), Val(3), Leu(6) and Val(8) could be shielded from the radical, the behavior of Val(2) and Val(7) was unanticipated. A possible interpretation for this observation is that the NH groups in extended strand conformations are in close proximity to CO groups of the same residue, a feature which may result in both steric and electrostatic shielding of the NH groups from interaction with the oxygen atom of the aminoxyl radical. It does appear that the delineation of intramolecularly hydrogen-bonded groups by radical induced line broadening may be more reliable in the case of folded helical structures as compared to extended β-sheets. An interesting feature of the spectrum in $CDCl_3$ is the absence of any pronounced concentration dependence of NMR parameters. Studies carried out over the peptide concentration range from 0.2 to 24 mM revealed no concentration dependence of NH chemical shifts, suggesting that the aggregation effects are unimportant. The sharp resonances observed in the NMR spectra also precluded significant aggregation. In a related study in this laboratory it has been observed that dramatic line broadening effects due to aggregation in $CDCl_3$ are indeed observed for octapeptide analogs in which amino acid replacements have been made in the strand and turn segments of the hairpin. β-Hairpins of the type illustrated in Fig. 2 would indeed be expected to self associate in weakly hydrogen bonding solvents because of the presence of unsatisfied hydrogen-bond donor and acceptor groups on the outer face of the hairpin. The precise reason for the reluctance of peptide **1** to aggregate is unclear, although such a property has proved advantageous in conformational analysis in apolar solvents.

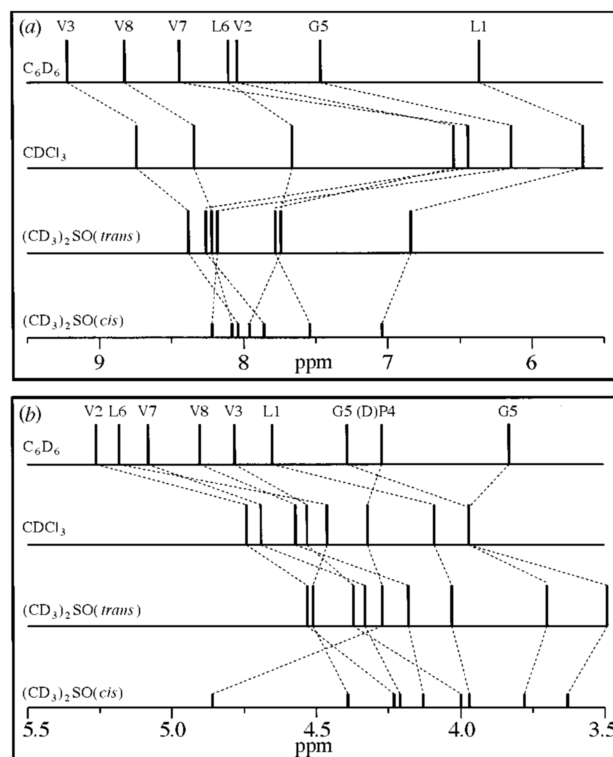

Fig. 4 Schematic representation of (*a*) NH and (*b*) CαH chemical shifts for peptide **1** (D-Pro-Gly) in C_6D_6, $CDCl_3$ and $(CD_3)_2SO$

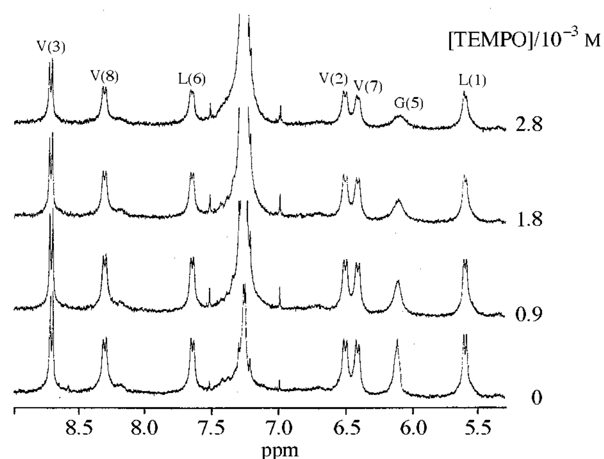

Fig. 5 Changes in linewidths of NH resonances in peptide **1** (D-Pro-Gly) upon addition of increasing concentrations of TEMPO in $CDCl_3$ solution. Peptide concentration, 8×10^{-3} M

Conformation in $(CD_3)_2SO$. The β-hairpin conformation (Fig. 2) of peptide **1** is stabilized by four intramolecular, interstrand hydrogen bonds. While such internal interactions are

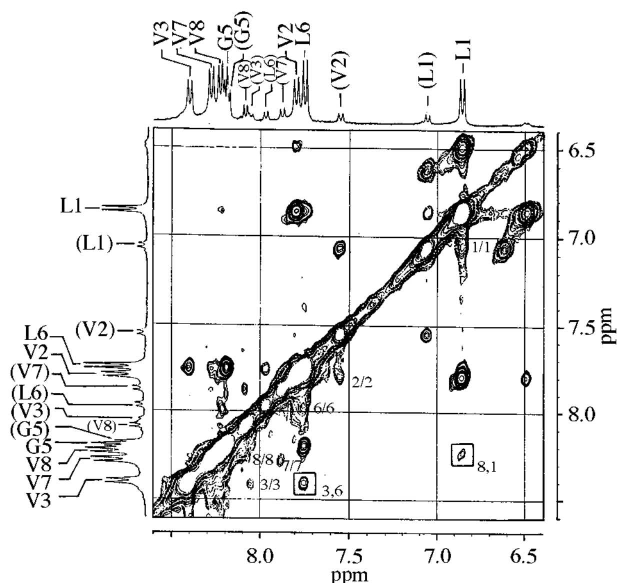

Fig. 6 Partial ROESY spectrum (400 MHz) of the NH–NH region, of peptide **1** (D-Pro-Gly) in $(CD_3)_2SO$. Minor resonances are indicated in parentheses.

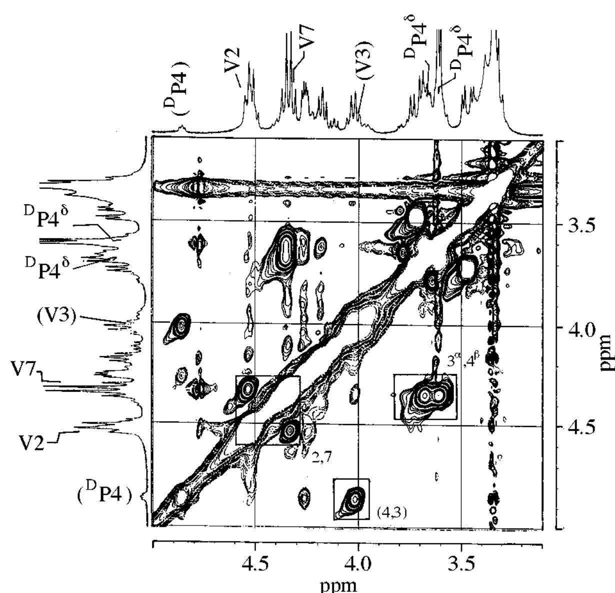

Fig. 7 Partial ROESY spectrum (400 MHz) of the $C^{\alpha}H$–$C^{\alpha}H$ region, of peptide **1** (D-Pro-Gly) in $(CD_3)_2SO$. Minor resonances are indicated in parentheses.

expected to be promoted in weakly hydrogen bonding solvents like C_6D_6 and $CDCl_3$, in more strongly solvated media an opening of the structure may be expected. The structure of peptide **1** was therefore investigated in $(CD_3)_2SO$. Two distinct conformations in slow exchange on the NMR timescale were observed in $(CD_3)_2SO$. Fig. 6 illustrates the presence of additional resonances, with a population distribution of 80% major and 20% minor species. The ROESY spectrum shown in Fig. 6 clearly establishes the presence of exchange cross peaks between the major and minor resonances. Fig. 7 shows a partial ROESY spectrum, which highlights $C^{\alpha}H\leftrightarrow C^{\alpha}H$ NOEs. The low-field Pro(4)$C^{\alpha}H$ (minor resonance) shows a NOE to Val(3)$C^{\alpha}H$ (minor resonance), confirming that the minor conformation arises due to the *cis* geometry about the Val(3)-D-Pro(4) peptide bond. Thus, the major conformation corresponds to the *trans* Val(3)-D-Pro(4) form. Assignments of all $C^{\alpha}H$ and NH resonances in both conformations were made on the basis of DQF-COSY and ROESY spectra in DMSO. NMR parameters for the backbone protons in DMSO are summarized in Table 1 and their chemical shifts are schematically compared in Fig. 4. A significant feature in $(CD_3)_2SO$ is the much smaller dispersion of NH chemical shifts in both conformations. This is unsurprising since all exposed NH resonances would be expected to move downfield due to solvent–solute hydrogen bonding. A comparison of $CDCl_3$ and $(CD_3)_2SO$ data in Fig. 4 suggests that the three internal NH groups Val(3), Val(8) and Leu(6) showed the smallest changes in chemical shifts on going from a polar solvent to a strongly solvating medium. An interesting feature of the chemical shifts in Fig. 4 is the large downfield shift of D-Pro(4)$C^{\alpha}H$ in the *cis* conformation.

Conformation of the trans form in $(CD_3)_2SO$.—The low temperature coefficient for Leu(6)NH supports the retention of the D-Pro-Gly β-turn conformation in $(CD_3)_2SO$. The observation of the Gly(5)/Leu(6) NH↔NH NOE and the D-Pro(4)/Gly(5) $C^{\alpha}H\leftrightarrow$NH NOE supports a type II′ conformation for this segment. The observation of the Val(3)↔Leu(6) and Leu(1)↔ Val(8) d_{NN} NOEs (Fig. 6) provides supporting evidence of the β-hairpin conformation shown in Fig. 2. Further support for the β-hairpin structure of the major conformation in $(CD_3)_2SO$ comes from a strong $d_{\alpha\alpha}$ NOE between Val(2)$C^{\alpha}H\leftrightarrow$Val(7)$C^{\alpha}H$ protons. These results together with the observed strong interresidue $C^{\alpha}_{i}H\leftrightarrow N_{i+1}H$ ($d_{\alpha N}$) NOEs for the segments 1–3 and 6–8 (Fig. 8) and the high $^3J_{NH\text{-}C^{\alpha}H}$ value at all Leu/Val residues (>8 Hz) provide unambiguous support for the β-hairpin structure.

Conformation of the cis form in $(CD_3)_2SO$.—In the *cis* form, although the NH resonances show limited chemical shift dispersion, there is a wide spread of $C^{\alpha}H$ resonances (Fig. 4). All the Leu/Val residues have high $^3J_{NH\text{-}C^{\alpha}H}$ values, indicating a preponderance of extended conformations for the segments 1–3 and 6–8. The high $d\delta/dt$ value of the Leu(6)NH clearly indicates the absence of the D-Pro-Gly β-turn. The characteristic interstrand NOEs observed in the *trans* form are also missing in the minor *cis* conformation. Isomerization about Val(3)-D-Pro(4) bond must result in an open, largely extended structure which may be extensively solvated.

NMR study of Boc-Leu-Val-Val-Pro-Gly-Leu-Val-Val-OMe 2

400 MHz ^{1}H NMR spectra of **2** in $CDCl_3$ at a concentration of 8 mM revealed very broad NH and $C^{\alpha}H$ resonances and sharp resonances for the side-chain methyl protons and *tert*-butyl protons of the Boc protecting groups (data not shown). The selective line broadening of the resonances of the backbone protons suggests formation of large peptide aggregates with relatively fast segmental motion of the side-chains. Upon addition of $(CD_3)_2SO$ to $CDCl_3$, line narrowing is observed, suggesting disruption of hydrogen-bonded aggregates due to competition with the solvent $(CD_3)_2SO$. In $(CD_3)_2SO$, sharp, well-resolved resonances were observed for the peptide **2**, suggesting the absence of pronounced aggregation effects in this solvent. In contrast to the D-Pro-Gly peptide **1**, only one set of NH and $C^{\alpha}H$ resonances is observed for the Pro-Gly peptide **2** in $(CD_3)_2SO$. The assignment of NH and $C^{\alpha}H$ resonances is achieved in a straightforward manner using a combination of DQFCOSY and ROESY methods. NMR parameters are summarized in Table 1. The $^3J_{NH\text{-}C^{\alpha}H}$ coupling constants are consistent with extended strand conformations at the 1–3 and 6–8 segments. The low $d\delta/dt$ value for Leu(6)NH is suggestive of solvent shielding. The strong Val(3) $C^{\alpha}H\leftrightarrow$Pro(4)$C^{\delta}H_2$ NOEs confirm the *trans* geometry of the Val-Pro bond. A comparison of the intensity of the NH↔NH NOEs in Fig. 9 with NH↔$C^{\alpha}H$ NOEs in Fig. 10 reveal that the latter are significantly more intense than the former. Interestingly, several sequential NH↔NH NOEs 1↔2↔3 and 6↔7↔8 were observed in peptide **2**. No interstrand NH↔NH and $C^{\alpha}H\leftrightarrow$ $C^{\alpha}H$ NOEs could be detected. The strong Pro(4)$C^{\alpha}H\leftrightarrow$Gly(5)-NH NOE together with the Gly(5)$C^{\alpha}H\leftrightarrow$Leu(6)NH NOE suggests a Type II β-turn centered at the Pro(4)-Gly(5) segment. This suggests that although a population of Pro-Gly Type II

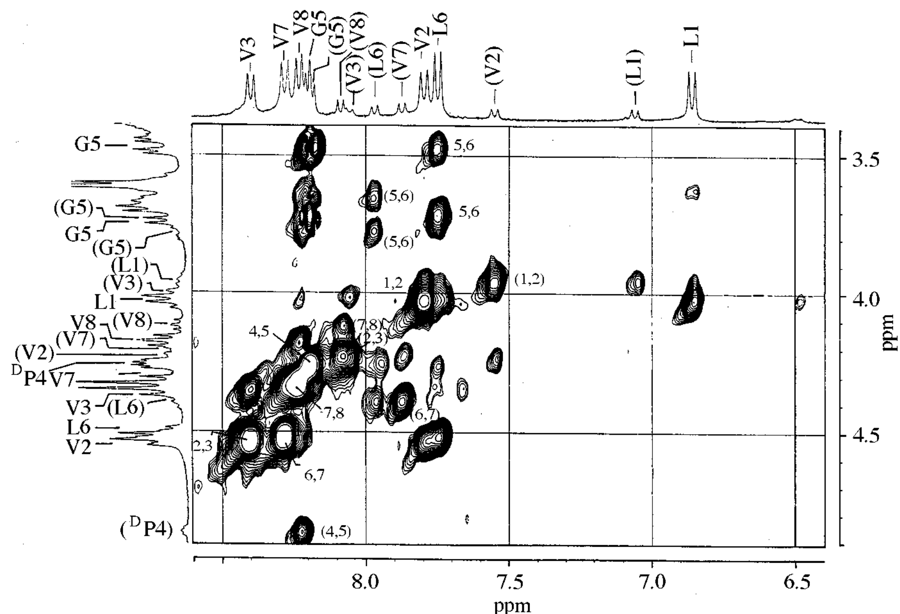

Fig. 8 Partial ROESY spectrum (400 MHz) of the C$^{\alpha}$H–NH region, of peptide **1** (D-Pro-Gly) in $(CD_3)_2SO$

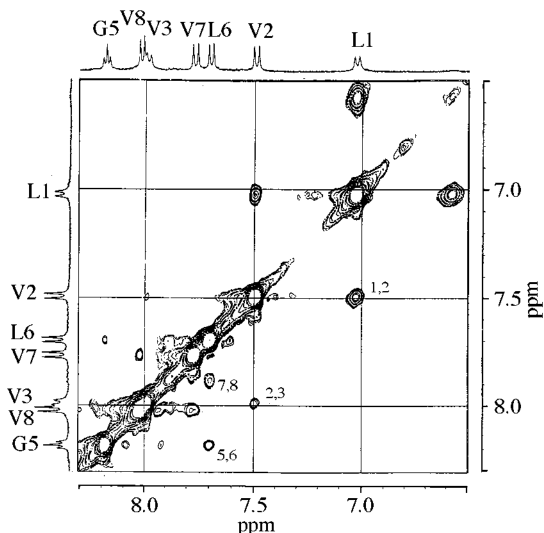

Fig. 9 Partial ROESY spectrum (400 MHz) of the NH–NH region, of peptide **2** (Pro-Gly) in $(CD_3)_2SO$

β-turn conformations may be present, the β-hairpin conformation is not obtained, with the two strands being highly solvated.

Circular dichroism comparison of peptides 1 and 2

The CD spectra of the two peptides in methanol are compared in Fig. 11. The D-Pro-Gly peptide **1** shows a characteristic negative band at 216 nm indicative of a β-hairpin conformation. This CD spectrum is maintained in diverse solvents, *e.g.* trifluroethanol, methanol and trimethylphosphate. Several well-defined water soluble β-hairpins[3,29,30] and β-sheet peptides[31–35] have also been reported to give a single negative band, with peak positions ranging from 214–218 nm. The CD spectrum of the Pro-Gly peptide **2** in methanol shows a red shift (221 nm) with diminished intensity suggesting a significant conformational difference from β-hairpin peptide **1**.

NMR derived structure for peptide 1

A model of peptide **1** was built on a SGI-INDIGO (II) workstation using the BIOSYM(Insight II) software package. The starting structure had ideal torsion angles of $\varphi = -120°$ and $\psi = 120°$ for Leu and Val residues with extended arms. The D-Pro-Gly segment was an ideal type II′ ($\varphi_{i+1} = 60°$, $\psi_{i+1} = -120°$, $\varphi_{i+2} = -80°$, $\psi_{i+2} = 0°$) β-turn. All peptide bonds including the Val-Pro residue were maintained in the *trans* form ($\omega = 180°$). To remove short contacts in the model, a 100 step steepest descent energy minimization was carried out. Sixteen distance constraints made up of six C$^{\alpha}$H–NH, three NH–NH, two C$^{\alpha}$H–C$^{\delta}$H, one C$^{\alpha}$H–C$^{\alpha}$H and four N–O distances were used in a 20 ps restrained molecular dynamics calculation *in vacuo*. Twenty structures separated by equal intervals of time were collected and used for further analysis. Fig. 12 shows the superposition of backbone atoms of these 20 structures maintaining the hairpin structure throughout. Average φ,ψ torsion angles are Leu(1) = −117°, 117°; Val(2) = −85°, 115°; Val(3) = −114°, 99°; D-Pro(4) = 70°, −8°; Gly(5) = −123°, 34°; Leu(6) = −125°, 123°, Val(7) = −96°, 113°; Val(8) = −104°, 113°.

Conclusions

The successful design of a stable β-hairpin in an apolar octapeptide **1** has been achieved using a centrally positioned D-Pro-Gly segment to nucleate a Type II′ β-turn. The stability of this β-hairpin conformation in crystals[23] and diverse organic solvents suggests that hairpin modules may become readily available for incorporation into synthetic sequences. The L-Pro-Gly peptide **2** does not adopt a β-hairpin conformation despite the presence of a Pro-Gly β-turn. Early analysis of β-hairpin structures in proteins reveals that Type I′/II′ turns, both of which have positive φ_{i+1} values, are favoured at the hairpin turn positions.[1,2] A more recent analysis with a larger protein data set suggests that β-hairpins nucleated by Type II β-turns are indeed found in proteins. However, strand links in these cases are significantly longer than the average hydrogen-bonded hairpin.[11] The ability to construct preorganized elements of secondary structure like β-hairpins[22,23] and helices[17–19] should facilitate modular construction of synthetic protein mimics. Although several recent investigations have focussed on the use of non-peptide templates for hairpin nucleation,[29,30,35–40] the use of conformationally constrained amino acid segments offer decided synthetic advantages.

Experimental

Materials and methods

The peptides were synthesized by classical solution phase procedures using a racemization-free fragment condensation strategy involving a final 3 + 5 coupling. The *tert*-butoxycarbonyl

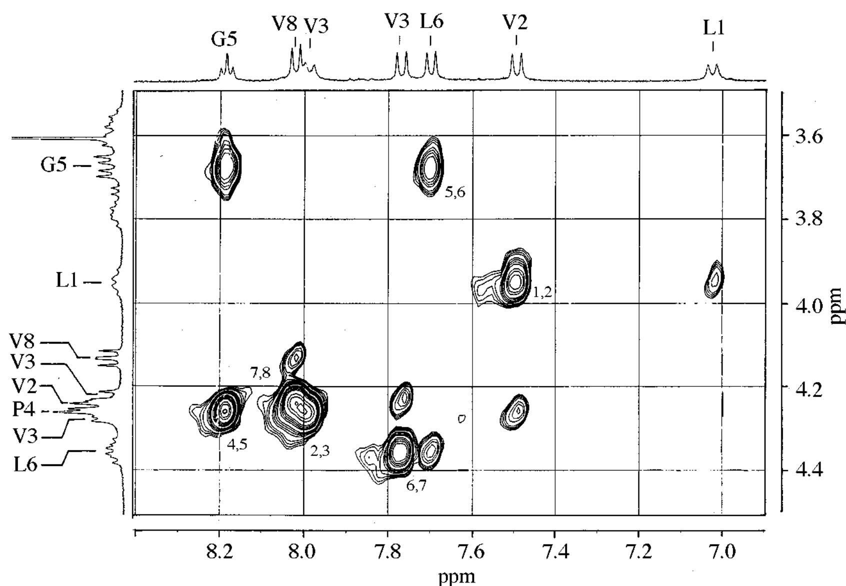

Fig. 10 Partial ROESY spectrum (400 MHz) of the C$^{\alpha}$H–NH region, of peptide **2** (Pro-Gly) in $(CD_3)_2SO$

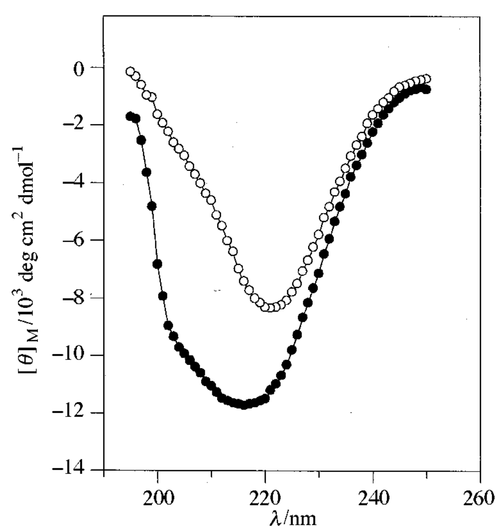

Fig. 11 Comparison of CD spectra of peptides **1** (●) and **2** (○) in methanol (concentration of the peptides in methanol: 2.7×10^{-4} mmol)

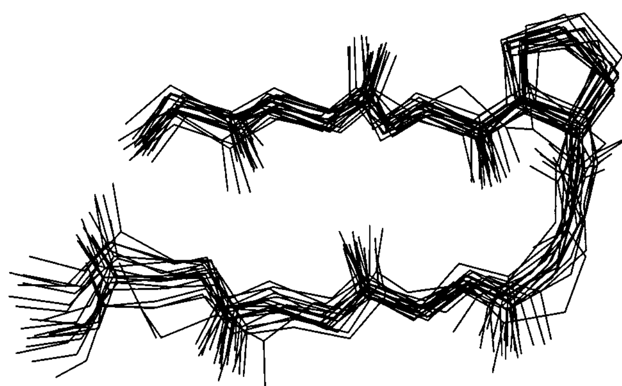

Fig. 12 Superposition of 20 structures collected at equal intervals of a 20 ps restrained molecular dynamics run using NMR derived restraints. Only traces of backbone atoms with the D-Pro ring are shown for clarity.

(Boc) group was used for *N*-terminal protection and the *C*-terminal was protected as a methyl ester (OMe). Deprotection was achieved by 98% formic acid or saponification, respectively. All intermediates were characterised by ^{1}H NMR spectroscopy (80 MHz) and thin layer chromatography (TLC) on silica gel. These intermediates were used without further purification. Peptides were purified by medium pressure liquid chromatography (MPLC) on a C_{18} (40–60 μm) column using methanol–water gradient elution. Representative solution phase synthetic procedures have been described elsewhere.[41] The peptides were characterized by complete assignment of the 400 MHz ^{1}H NMR spectra.

Resonance assignments were made using DQFCOSY and ROESY spectra. All 2D experiments were recorded in phase sensitive mode by using the time proportional phase incrementation method (TPPI). 1024 and 512 data points were used in t_2 and t_1 dimensions, respectively. The resultant data set was zero filled to finally yield 1 × 1 K data points. A shifted square sine bell window was used in both dimensions. Spectral widths were in the range of 4500 Hz. Peptide concentration was 7–8 mM and the probe temperature was maintained at 298 K. CD spectra were recorded on JASCO-500 spectropolarimeter using 1 mm pathlength cuvettes.

References

1 B. L. Sibanda and J. M. Thornton, *Nature* (*London*), 1985, **316**, 170.
2 B. L. Sibanda, T. L. Blundell and J. M. Thornton, *J. Mol. Biol.*, 1989, **206**, 759.
3 M. R. Alvarado, F. J. Blanco and L. Serrano, *Nat. Struct. Biol.*, 1996, **3**, 604.
4 M. S. Searle, R. Zerella, D. H. Williams and L. C. Packman, *Protein Eng.*, 1996, **9**, 559.
5 V. Sieber and G. R. Moe, *Biochemistry*, 1996, **35**, 181.
6 R. L. Fahner, T. Dieckmann, S. S. L. Harwing, R. L. Lehrer and D. Eisenberg, *J. Chem. Biol.*, 1996, **3**, 543.
7 T. S. Haque and S. H. Gellman, *J. Am. Chem. Soc.*, 1997, **119**, 2303.
8 E. D. Alba, M. A. Jiminez and M. Rico, *J. Am. Chem. Soc.*, 1997, **119**, 175.
9 E. D. Alba, F. J. Blanco, M. A. Jiminez, M. Rico and J. L. Nieto, *Eur. J. Biochem.*, 1995, **233**, 283.
10 M. S. Searle, D. H. Williams and L. C. Packman, *Nat. Struct. Biol.*, 1995, **2**, 999.
11 K. Gunasekaran, C. Ramakrishnan and P. Balaram, *Protein Eng.*, 1997, in the press.
12 C. M. Venkatachalam, *Biopolymers*, 1968, **6**, 1425.
13 C. M. Wilmot and J. M. Thornton, *J. Mol. Biol.*, 1988, **203**, 221.
14 P. Y. Chou and G. D. Fasman, *J. Mol. Biol.*, 1997, **115**, 135.
15 J. S. Richardson, *Adv. Protein Chem.*, 1981, **34**, 167.
16 N. Srinivasan, V. S. Anuradha, C. Ramakrishnan, R. Sowdhamini and P. Balaram, *Int. J. Pept. Protein Res.*, 1994, **44**, 112.
17 W. F. DeGrado, *Adv. Protein Chem.*, 1988, **39**, 51.
18 P. Balaram, *Pure Appl, Chem.*, 1992, **64**, 106.
19 M. D. Struthers, R. P. Cheng and B. Imperiali, *Science*, 1996, **271**, 342.
20 T. S. Haque, J. C. Little and S. H. Gellman, *J. Am. Chem. Soc.*, 1994, **116**, 105.

21 T. S. Haque, J. C. Little and S. H. Gellman, *J. Am. Chem. Soc.*, 1996, **118**, 6975.
22 S. K. Awasthi, S. Raghothama and P. Balaram, *Biochem. Biophys. Res. Commun.*, 1995, **216**, 375.
23 I. L. Karle, S. K. Awasthi and P. Balaram, *Proc. Natl. Acad. Sci. USA.*, 1996, **93**, 8189.
24 K. Wuthrich, *NMR of Proteins and Nucleic acids*, Wiley, New York, 1986.
25 Y. V. Venkatachalapati and P. Balaram, *Biopolymers*, 1981, **20**, 625.
26 M. Iqbal and P. Balaram, *J. Am. Chem. Soc.*, 1981, **103**, 5548.
27 K. D. Kopple and T. J. Schamper, *J. Am. Chem. Soc.*, 1972, **94**, 3644.
28 K. D. Kopple, A. Go and D. R. Pilipauskas, *J. Am. Chem. Soc.*, 1975, **97**, 6830.
29 C. L. Nesloney and J. W. Kelly, *J. Am. Chem. Soc.*, 1996, **118**, 5836.
30 J. P. Schneider and J. W. Kelly, *J. Am. Chem. Soc.*, 1995, **117**, 533.
31 E. K. Krause, M. Beyermann, H. Fabian, M. Dathe, S. Rothemund and M. Bienert, *Int. J. Pept. Protein Res.*, 1996, **48**, 559.
32 J. Reed and V. Kinzel, *Biochemistry*, 1991, **30**, 4521.
33 K. H. Mayo, E. Ilyina and H. Park, *Protein Sci.*, 1996, **5**, 1301.
34 S. Zhang and A. Rich, *Proc. Natl. Acad. Sci. USA.*, 1997, **94**, 23.
35 Y. Fukushima, *Bull. Chem. Soc. Jpn.*, 1996, **69**, 701.
36 J. M. Nowick, D. L. Holmes, G. Mickin, G. Noronha, A. J. Shaka and E. M. Smith, *J. Am. Chem. Soc.*, 1996, **118**, 2764.
37 K. McWilliams and J. W. Kelly, *J. Org. Chem.*, 1996, **61**, 7408.
38 K. Y. Tsang, H. G. Diaz, N. Graciani and J. W. Kelly, *J. Am. Chem. Soc.*, 1994, **116**, 3988 and references cited therein.
39 A. B. Smith II, M. C. Guzman, P. A. Sprengeler, T. P. Keenan, R. C. Holcomb, J. L. Wood, P. J. Carrol and R. Hirschmann, *J. Am. Chem. Soc.*, 1994, **116**, 9947.
40 D. S. Kemp, B. R. Bowen and C. C. Muendel, *J. Org. Chem.*, 1994, **55**, 4650.
41 S. K. Awasthi, S. R. Raghothama and P. Balaram, *J. Chem. Soc., Perkin Trans. 2*, 1996, 2701.

Paper 7/03331A
Received 13*th May* 1977
Accepted 15*th August* 1977